Constraining Southern Ocean CO_2 Flux Uncertainty Using Uncrewed Surface Vehicle Observations

A. J. Sutton[1] , **N. L. Williams[2]** , and **B. Tilbrook[3,4]**

[1]Pacific Marine Environmental Laboratory, National Oceanic and Atmospheric Administration, Seattle, WA, USA, [2]University of South Florida, St. Petersburg, FL, USA, [3]Oceans and Atmosphere, Commonwealth Scientific and Industrial Research Organisation, Hobart, TAS, Australia, [4]Australian Antarctic Program Partnership, University of Tasmania, Hobart, Australia

Abstract Remote, harsh conditions of the Southern Ocean challenge our ability to observe the region's influence on the climate system. Southern Ocean air-sea CO_2 flux estimates have significant uncertainty due to the reliance on limited ship-dependent observations in combination with satellite-based and interpolated data products. We utilize a new approach, making direct measurements of air-sea CO_2, wind speed, and surface ocean properties on an Uncrewed Surface Vehicle (USV). In 2019, the USV completed the first autonomous circumnavigation of Antarctica providing hourly CO_2 flux estimates. Using this unique data set to constrain potential error in different measurements and propagate those through the CO_2 flux calculation, we find that different wind speed products and sampling frequencies have the largest impact on CO_2 flux estimates with biases that range from −4% to +20%. These biases and poorly constrained interannual variability could account for discrepancies between different approaches to estimating Southern Ocean CO_2 uptake.

Plain Language Summary The Southern Ocean is an important part of the global climate, playing an outsized role in the uptake of heat and carbon. Yet observing the Southern Ocean is challenging due to its size, remoteness, and harsh conditions. In 2019, we completed the first autonomous circumnavigation of Antarctica with an Uncrewed Surface Vehicle (USV), also known as an ocean robot, in order to address some of these observing challenges. By directly measuring air and surface seawater carbon dioxide (CO_2) and wind speed on the USV, we were able to observe CO_2 exchange between the ocean and atmosphere every hour during the mission. Using this data set, we estimated potential errors in these measurements as well as other approaches to estimating CO_2 exchange. The use of different satellite-based wind products and sampling frequency play the largest role in uncertainty of the uptake of CO_2 in the Southern Ocean. In order to reduce this uncertainty and provide a better understanding of the Southern Ocean, expansion of an observing network made up of ships, USVs, and other autonomous devices is necessary.

1. Introduction

Covering only 30% of the global ocean surface, the Southern Ocean (most often defined as south of 30°S–35°S) plays an outsized role in the climate system. It is the meeting point of ocean currents and a connector between the atmosphere and ocean interior for the transfer of heat and carbon, accounting for as much as 75% and 40% of global ocean heat and carbon uptake, respectively (Frölicher et al., 2014; Khatiwala et al., 2009). While questions remain as to all of the mechanisms that contribute to CO_2 flux and the over-turning circulation in the Southern Ocean, it is becoming clear that control of net CO_2 uptake over annual to decadal scales is dominated by wind-driven physical mixing and upwelling of carbon-rich deep water (Iudicone et al., 2011; Lovenduski et al., 2008).

Southern Ocean CO_2 flux is primarily a balance between the outgassing of natural carbon in upwelled waters not taken up by biological processes and the flux of anthropogenic carbon into the ocean driven by increasing atmospheric CO_2. These processes occur continuously and simultaneously as cold, carbon-rich water outgasses in upwelling regimes, and absorbs anthropogenic heat and carbon as the water flows north in the surface layer to warmer regimes. These processes vary across the diversity of Southern Ocean regimes

from the temperature-dominated system in the Subtropical Zone to the sea ice- and biologically dominated regime closest to Antarctica.

The combination of these diverse and variable biogeochemical regimes, sparse observations, and inadequate constraint of circulation in models challenge estimates of Southern Ocean CO_2 uptake. Climatological mean uptake estimates based on observations from ships range from -0.8 to -1.0 Pg C yr^{-1} (Landschützer et al., 2014; Takahashi et al., 2009). While the magnitude of interannual variability is unknown, the temporal variability of CO_2 flux at interannual to decadal time scales is correlated with atmospheric variability as defined by the Southern Annular Mode (SAM) index: the difference in mean sea level pressure between 40°S and 65°S (Marshall, 2003). When the SAM index is positive, winds south of 45°S increase, potentially accelerating upwelling of carbon-rich deep water and reducing net CO_2 uptake. A negative SAM index is associated with a reduction of both upwelling and ventilation of CO_2 to the atmosphere, allowing increased net CO_2 uptake. However, there are regional variations in CO_2 flux response to SAM conditions that are not fully understood (Keppler & Landschützer, 2019; Nevison et al., 2020). Keppler and Landschützer (2019), for example, found increased upwelling and CO_2 outgassing in higher latitudes during positive SAM conditions but opposing effects in other regions. Several data- (Fay et al., 2014; Landschützer et al., 2015; Takahashi et al., 2012) and modeling-based (Le Quéré et al., 2007; Lovenduski et al., 2007, 2008, 2015) studies suggest decadal-scale variability of Southern Ocean CO_2 uptake is within ± 0.4 Pg C yr^{-1}, a significant portion of the climatological mean estimate of -0.8 to -1.0 Pg C yr^{-1}.

New observations, however, challenge whether the Southern Ocean is a strong sink. Biogeochemical float data from 2014–2017 estimate a Southern Ocean CO_2 flux of -0.08 Pg C yr^{-1} (Gray et al., 2018), an order of magnitude less than the climatological mean estimates based on ship-based surface ocean CO_2 partial pressure (pCO$_2$) data products (Landschützer et al., 2014, 2016; Rödenbeck et al., 2015; Takahashi et al., 2009). Even after correcting for a potential bias of 4 μatm to the float-based calculated seawater pCO$_2$, discrepancies between ship- and float-based CO_2 flux estimates remain (Bushinsky et al., 2019). Whether recent float-based CO_2 flux estimates represent an updated understanding of the climatological mean, float-based seawater pCO$_2$ requires an even larger bias correction, or 2014–2017 conditions were anomalous, is currently unresolved.
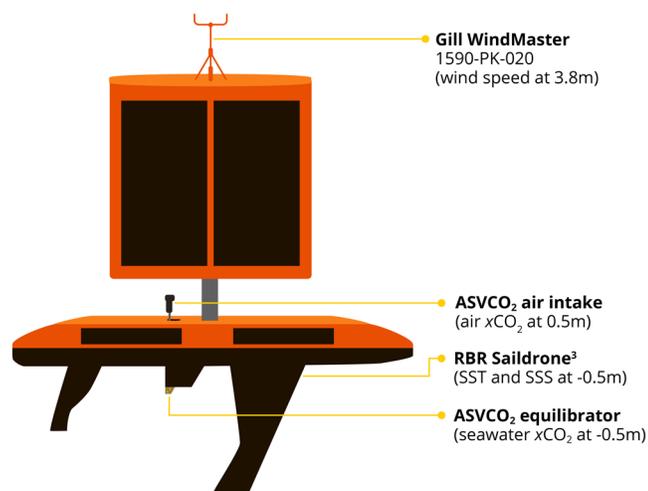
A criticism of ship-based estimates is the scarcity of data in both time and space, especially during winter months. However, surface ocean pCO$_2$ is measured directly on ships with low uncertainty ($\pm 0.5\%$) (Pierrot et al., 2009), compared to pCO$_2$ calculated from float pH measurements and estimated total alkalinity that has a higher uncertainty ($\pm 2.8\%$) (Bushinsky et al., 2019; Williams et al., 2017). Unlike ships, floats are able to sample in harsh winter conditions unfit for safe ship operations as well as under ice, increasing the potential for filling observational gaps. Another issue impacting the uncertainty in both float- and ship-based climatological CO_2 flux estimates is the use of observation-derived atmospheric CO_2 products and satellite-based wind and sea level pressure products, which have been shown to add significant uncertainty to CO_2 flux estimates in some regions (Chiodi et al., 2019; Roobaert et al., 2018; Sutton et al., 2017).

Technological advances of Uncrewed Surface Vehicles (USVs) address these observational challenges through remote surveying in harsh conditions with direct measurements of air-sea pCO$_2$ and wind speed. Here we present results from the first autonomous circumnavigation of Antarctica, a 22,000-km, 196-day mission. A Saildrone Inc. USV with an integrated Autonomous Surface Vehicle CO_2 (ASVCO$_2$™) system was designed specifically to survive the forces of being rolled and submerged by 15-m breaking waves in the Southern Ocean. We calculate air-sea CO_2 flux from the USV and provide a thorough comparison of potential bias in CO_2 flux calculated with direct measurements relative to recent float-based methods (Bushinsky et al., 2019; Gray et al., 2018) and a ship-based data product (Landschü;tzer et al., 2020) that rely on other satellite- and observational-based data products. We then discuss the potential role of flux uncertainty and interannual variability in determining the Southern Ocean carbon sink.

2. Materials and Methods

2.1. USV and Sensors

The Saildrone USV is an ocean-going drone navigable via satellite communications with wind-driven propulsion and primarily solar-powered meteorological and surface ocean physical, chemical, and bio-

Gill WindMaster
1590-PK-020
(wind speed at 3.8m)

ASVCO$_2$ air intake
(air xCO$_2$ at 0.5m)

RBR Saildrone^3
(SST and SSS at -0.5m)

ASVCO$_2$ equilibrator
(seawater xCO$_2$ at -0.5m)

Figure 1. Schematic diagram of the 2019 Southern Ocean Saildrone Uncrewed Surface Vehicle (USV) and location of the sensors used in this study. Schematic is not to scale.

logical sensors. The Saildrone USV that completed the 2019 Antarctica circumnavigation is similar to the standard vehicles with a 7 m hull and 2.5 m keel described by Meinig et al. (2019) and Zhang et al. (2019) but includes an adapted wing to survive the extreme, high winds and waves of the Southern Ocean (Figure 1). This USV design includes a lower-aspect square rig designed to withstand the force of being rolled and submerged by 15 m breaking waves but limits navigation to sailing primarily downwind. This design has been recently modified to improve maneuverability.

Meteorological sensors are mounted on the square wing, including a Gill WindMaster™ anemometer at 3.8 m height. Through field intercomparisons, Zhang et al. (2019) found RMS differences of ±0.6−1.0 m s^{-1} between wind speed measured on Saildrone USVs with the standard 5 m wing compared to both the Woods Hole Oceanographic Institute's buoy Air-Sea Interaction METeorology System and the R/V *Revelle*. In this study, we use the higher-bound wind speed error of ±1.0 m s^{-1} derived by Zhang et al. (2019) for the estimated error of wind speed measured from the shorter wing at 3.8 m. Even though they determined that bias was inconclusive, to generate conservative estimates we use the mean bias determined from Zhang et al. (2019) intercomparisons of +0.2 m s^{-1}.

The ASVCO$_2$™ system is packaged in a waterproof enclosure mounted in the USV hull. The ASVCO$_2$ is nearly identical to the Moored Autonomous pCO$_2$ (MAPCO$_2$™) system that has been used for over 2 decades on dozens of surface buoys and has a lab- and field-validated uncertainty of ±2 µatm or ±0.5% (Sabine et al., 2020; Sutton et al., 2014). These CO$_2$ systems utilize an equilibrator-based gas collection system and an infrared gas analyzer (LI-820, LI-COR™) calibrated in situ with reference gas traceable to World Meteorological Organization standards, a similar methodology to the underway pCO$_2$ system deployed on the global network of ships of opportunity (Pierrot et al., 2009). In order to adapt the MAPCO$_2$ for USV deployments, the ASVCO$_2$ includes an equilibrator mounted to the USV hull with a fairing added to maintain consistent water level in the equilibrator when moving at speeds greater than four knots (Figure 1).

The ASVCO$_2$ system collects 1-hourly measurements of sea surface and marine boundary layer atmospheric xCO$_2$ (the mole fraction of CO$_2$) and sea level atmospheric pressure. Each xCO$_2$ measurement is paired with sea surface temperature (SST) and salinity (SSS) collected by an RBR Saildrone^3 CTD customized for mounting through the Saildrone USV keel at 0.5 m depth. Seawater and air pCO$_2$ (at in situ SST) is calculated according to standard operating procedures (Dickson et al., 2007; Weiss, 1974) as described in Sutton et al. (2014). Data from the ASVCO$_2$ system and wind speed, SST, and SSS are archived at the National Centers for Environmental Information (Sutton et al., 2020).

The USV was deployed from Bluff, New Zealand on January 19, 2019. Sailing downwind, the USV navigated east 22,000 km around Antarctica and was recovered off Bluff on August 3, 2019, 196 days later. The anemometer was damaged near the Drake Passage during an iceberg collision at the end of March.

2.2. Comparison Data Sets

Several data sets are used as comparisons for the USV-derived CO$_2$ fluxes. The first is v2020 of the SOM-FFN neural network product documented in Landschützer et al. (2016), which uses ship-based measurements of seawater pCO$_2$ to estimate monthly air-sea CO$_2$ fluxes globally over the period 1982 to 2019 (Landschü;tzer et al., 2020). The second product is the same SOM-FFN neural network, but with the addition of Southern Ocean Carbon and Climate Observations and Modeling project (SOCCOM) float-derived pCO$_2$ as training data sets (Bushinsky et al., 2019). This product is available as "SOCCOM-only" as well
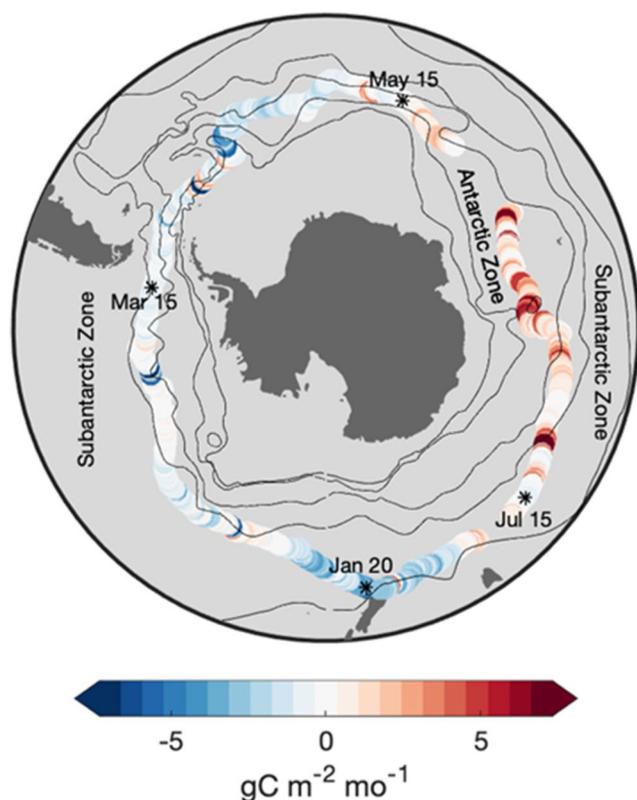
Figure 2. CO_2 flux calculated from Uncrewed Surface Vehicle (USV)-measured ΔpCO_2, sea surface temperature (SST), and salinity (SSS) and CCMP V2 wind speed. Dates and * show the location of the USV with time. Black lines indicate climatological locations of the major fronts from Orsi et al. (1995) as in Figure S1.

as "SOCCOM + ship" for the years 2014–2017. To compare these two data sets with the USV, we subsample each product at the location and month of each USV CO_2 flux measurement and average the CO_2 fluxes over 10-day periods.

The third comparison data set is air-sea CO_2 fluxes estimated from calculated surface ocean pCO_2 from SOCCOM biogeochemical float data from 2015 to 2019, which is available online as a quality-controlled data snapshot dated August 30, 2020 (Johnson et al., 2020). All float profiles from 2015 to 2019 were separated by year and front locations, and subsequently averaged by month to create monthly pCO_2 and CO_2 flux estimates for each of the three major zones discussed in this manuscript. The Subantarctic Zone is defined as profiles with an oxygen minimum deeper than 1,200 m, a salinity maximum deeper than 500 m, and surface waters fresher than 34.6. The Polar Frontal zone is defined as profiles with an oxygen minimum between 900 and 1,200 m deep and a deep (>1,400 m) salinity maximum. The Antarctic Zone is defined as profiles with an oxygen minimum between 600 and 900 m deep and a salinity maximum deeper than 1,000 m. While there are some profiles within the Seasonal Sea Ice Zone which fall within the definitions above, these profiles are not included in the analysis if they occur during a calendar year when that float profiled under ice. In contrast to previous studies, the float profiles have not been extrapolated over time and the monthly averages only represent averages of the instantaneous fluxes at the time of the float surfacing.

We use CO_2 flux provided by the first two comparison data sets (Bushinsky et al., 2019; Landschützer et al., 2020). CO_2 flux for the third comparison data set (SOCCOM biogeochemical floats from 2015 to 2019) and the USV are calculated using established methodologies summarized in the Supplemental.

3. Results and Discussion

3.1. Air-Sea Observations

During the mission, the USV observed a large range in ΔpCO_2 (seawater-air pCO_2) of 33 to −40 μatm with a slightly negative mean of −4 μatm and a variance of ±12 μatm (Figure 2). Although periods of negative and positive ΔpCO_2 were observed throughout the deployment, positive ΔpCO_2 indicating outgassing was prevalent during the latter part of the deployment, primarily during late fall and early winter in the Indian Ocean sector of the Antarctic Zone (Figure S1). Observed mean, variation, and range of air xCO_2, sea pCO_2, ΔpCO_2, SST, SSS, and wind speed are given in Table S2.

3.2. CO_2 flux Uncertainty Analysis

The uncertainty in calculated CO_2 flux can vary widely given the different options of inputs. The gas transfer velocity (k) uncertainty of 20% applies to all CO_2 flux estimates (Wanninkhof, 2014), leaving the choice and availability of wind speed, seawater pCO_2, and air pCO_2 data sets the major sources of variation among different approaches.

Given the scarcity of in situ wind speed observations, the use of satellite-based wind speed in calculating CO_2 flux is common. However, in many regions, these satellite-based products have biases in comparison to available in situ data (Hihara et al., 2015; Kent et al., 2013; Tomita et al., 2015; Wallcraft et al., 2009; Weissman et al., 2012) and can have significant impacts on CO_2 flux estimates (Chiodi et al., 2019; Roobaert et al., 2018; Sutton et al., 2017). Directly measured wind speed also suffer errors due to flow distortion, plat-

Table 1
Estimated Bias for Different Approaches of Calculating CO$_2$ Flux by Applying Mean Bias From S1 to Conditions Observed During the 2019 USV Deployment

Seawater pCO$_2$ data source	Air pCO$_2$ data source	Wind speed data source	Estimated CO$_2$ flux bias
USV	USV	USV	−4%
Ship or USV	Ship, USV, MBL, or Gape Grim	CCMP V2 or ERA-Interim	−4%
Float-derived	MBL or Cape Grim	ERA-Interim	+20%

Notes. Resulting biases are additive based on mean biases reported in Table S1. A negative bias suggests less outgassing/more uptake; positive suggests more outgassing/less uptake. The USV CO2 flux bias results from the estimated USV wind speed bias of +0.2 m s^{-1} (Zhang et al., 2019).
Abbreviations: MBL, Marine Boundary Layer; USV, Uncrewed Surface Vehicle.

form movement, and wave shadowing, resulting in uncertainties of ±0.1 m s^{-1} on buoys (Cronin et al., 2008; Kubota et al., 2008; Weller, 2015) and up to ±1.0 m s^{-1} on Saildrone USVs (Zhang et al., 2019).

Prior to the USV anemometer being damaged in March 2019, there is no mean difference between USV-measured and Cross-Calibrated MultiPlatform Near Real Time V2.0 (CCMP V2) wind speed (Mears et al., 2019) or ERA-Interim Reanalysis (Dee et al., 2011) wind speed with a variance around wind speed residuals of ±1.8 m s^{-1} and ±2.0 m s^{-1}, respectively (Figure S2). NCEP-DOE AMIP-II Reanalysis 2 (NCEP-2) (Kanamitsu et al., 2002) and ERA5 (Hersbach et al., 2020) wind speeds have lower wind speed by 1.0 and 0.1 m s^{-1}, respectively, than measured on the USV with a variance around the mean bias of ±3.9 and ± 1.4 m s^{-1}, respectively. In Table S1 these biases are reported relative to the "true" wind speed by correcting for the USV wind speed bias of +0.2 m s^{-1} (Zhang et al., 2019). Importantly, the biases in satellite-based wind speed products relative to the USV-measured wind speed are not randomly distributed. Satellite and USV wind speeds tend to agree most closely at wind speeds of 10 m s^{-1}, but diverge at lower and higher wind speeds (Figure S2c). These results are consistent with biases reported in other intercomparisons mentioned previously and summarized by Cronin et al. (2019).

Uncertainties associated with ship-, USV-, and float-based sources of pCO$_2$ are ±0.5%, ±0.5%, and ±2.8%, respectively (Table S1.) Common data sources of atmospheric baseline xCO$_2$ are the NOAA Greenhouse Gas Marine Boundary Layer (MBL) Reference CO$_2$ product (Dlugokencky et al., 2019) or observations from nearby atmospheric observatories, like at Cape Grim. Monthly mean xCO$_2$ from these two sources and the USV tend to agree within 0.2 ppm; however, shorter-term variability indicating terrestrial biosphere influence is prevalent within the hourly USV observations (Figure S3) and the hourly in situ Cape Grim observations (data not shown). Converting these sources of xCO$_2$ to pCO$_2$ requires atmospheric pressure at sea level, which if using satellite-based products such as NCEP 2, ERA-Interim, or ERA5 introduces another possible source of error (Table S1).

Various sampling frequencies of these data sources can also introduce error into the CO$_2$ flux calculation. Monthly CO$_2$ flux calculated from subsampling the hourly USV ΔpCO$_2$ data set at 6-hourly intervals, which is the common temporal frequency of satellite-based products, results in nearly identical values to monthly flux calculated from the hourly observations (Figure S4). However, subsampling the hourly data set at all possible 10-day sampling frequencies, the timescale for float observations, results in an integrated bias in CO$_2$ flux of +0.05 g C m^{-2} mo^{-1} or +23% (less uptake/more outgassing) over the 7-month comparison period with large variation around the monthly means due to the high temporal variability of the data set at a scale of less than 10 days.

Propagated bias of USV-derived CO$_2$ flux is −4% (less outgassing/more uptake) driven by the potential bias in USV-measured wind speed (Table 1). In this case, USV, CCMP V2, and ERA-Interim wind speed bias are equivalent and have the same impact on calculated CO$_2$ flux. Replacing directly measured air pCO$_2$ with pCO$_2$ calculated from MBL or Cape Grim values and NCEP 2, ERA-Interim, or ERA5 sea level pressure does not significantly impact flux bias. Taking into consideration the potential bias of subsampling at 10-day intervals combined with the ERA-Interim wind speed bias results in an overall positive bias of +20% (more outgassing/less uptake) in calculated CO$_2$ flux primarily due to the bias in subsampling the 2019 USV
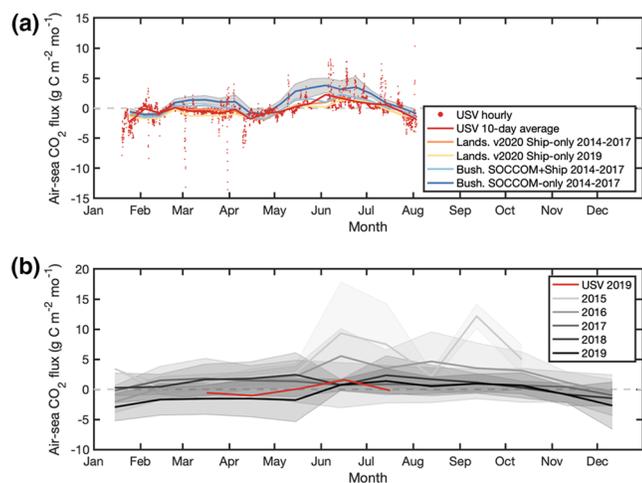
Figure 3. (a) Time series of monthly CO_2 flux calculated using all Uncrewed Surface Vehicle (USV) observations at hourly (red dots) and 10-day averaged (red line) time steps; from Landschützer et al. (2020) SOM-FFN ship-based climatology (orange) and 2019 (yellow) subsampled at the Saildrone locations and times and averaged over 10 days; and from Bushinsky et al. (2019) using the same methods of the SOM-FFN v2020 ship-based climatology for the years 2014–2017 but incorporating seawater pCO_2 estimated from both ships and Southern Ocean Carbon and Climate Observations and Modeling (SOCCOM) biogeochemical-float observations (light blue), and using only SOCCOM biogeochemical float observations (dark blue) for the years 2014–2017. The shaded area represents the interannual variability in the SOCCOM-only product over 2014–2017. (b) Antarctic Zone monthly averaged USV fluxes (red) plotted with monthly mean SOCCOM float-based CO_2 flux from 2015 to 2019 in that zone (gray). The shaded area is 1σ of monthly mean SOCCOM CO_2 flux.

data set at 10-day intervals. Monteiro et al. (2015) found that a 10-day sampling period in spring-summer in the Subantarctic Zone resulted in a 10%–25% increase in uncertainty in CO_2 flux relative to hourly sampling due to mixed layer responses to storm events, which may explain a similar magnitude sampling bias observed with the USV results.

3.3. CO$_2$ Flux Comparisons

Due to the loss of the wind speed sensor during the USV deployment, USV CO_2 flux presented in this section is calculated using CCMP V2 wind speed. During the 2019 circumnavigation, the USV observed periods of strong outgassing as high as $10.5 \, g \, C \, m^{-2} \, mo^{-1}$ in June and July in the Antarctic Zone, which was one of the zones where SOCCOM float-based data from 2014–2017 showed stronger outgassing than the SOM-FFN ship-based climatology (Figure 3a; Bushinsky et al., 2019; Gray et al., 2018). There were also periods of intense short-scale CO_2 uptake during February through April, some of which were associated with phytoplankton blooms (data not shown). The periods of strong outgassing observed by the USV in June and July overlap with the Bushinsky et al. (2019) 2014–2017 SOCCOM-only SOM-FFN estimates of CO_2 outgassing (Figure 3a). However, the USV observations show these outgassing events occur over time periods from hours to two days in length, and these short-lived outgassing events do not lead to outgassing as strong as the SOCCOM-only SOM-FFN estimates when averaged at the 10-day scale. Mean USV CO_2 flux in June and July results in a weak net outgassing of $0.7 \, g \, C \, m^{-2} \, mo^{-1}$, more similar to the Landschützer et al. (2020) ship-based data product and the Bushinsky et al. (2019) combined SOCCOM-ship SOM-FFN product than the SOCCOM-only SOM-FFN product.

Focusing only on 2019 observations, USV-measured and float-estimated surface seawater pCO_2 are consistent within standard deviations of monthly means within the Subantarctic Zone and the Antarctic Zone, the two major zones sampled by the 2019 Saildrone USV (Figure S5). Within the Antarctic Zone where Gray et al. (2018) found the largest winter-time discrepancy between float- and ship-based data, we find a mean difference of $0.5 \pm 2.6 \, g \, C \, m^{-2} \, mo^{-1}$ (or no significant difference) between USV and float-derived CO_2 flux in March through July 2019 (Figure 3b). To test the possible effect of variable float locations on the estimates of CO_2 flux in the Antarctic Zone, the Landschützer v2020 SOM-FFN ship-based climatology was subsampled at the times and locations of each float observation. Float-based fluxes are on average $1.5 \, g \, C \, m^{-2} \, mo^{-1}$ greater than the ship-based climatology in this zone for 2015–2019 with significant interannual variability (2015: +3.9, 2016: +2.1, 2017: +0.6, 2018: +0.8, and 2019: $-0.1 \, g \, C \, m^{-2} \, mo^{-1}$).

Figure 3b illustrates this significant interannual variability in float-derived CO_2 flux in the Antarctic Zone from 2015–2019. Net CO_2 uptake observed by the USV and floats in 2019 contrasts with the strong outgassing during winter of 2015 and 2016. This interannual variability may be influenced by SAM with increased westerly wind strength during the more positive phases of SAM increasing upwelling of relatively CO_2-rich waters. The greatest outgassing is observed in the Antarctic Zone during strong positive phases of SAM in 2015 and 2016 (Figure 3b and Figure S6). The USV data were collected during a decline in the SAM index and are similar to the float-based net flux estimates for 2019 (Figure 3b).

Analysis of the Saildrone USV observations reveal several potential sources of bias and error in USV-, ship-, and float-based CO_2 flux (Tables S1 and Table 1). Given the significant fine-scale temporal and spatial variability observed during 2019, the 10-day sampling routine of floats may introduce a bias (more outgassing/ less uptake in this case), which could account for some of the difference between float- and ship-based CO_2 flux reported previously (Bushinsky et al., 2019; Gray et al., 2018). It is also critical to better constrain how shifts in SAM conditions play a role in Southern Ocean CO_2 flux. The larger differences between the

ship-based climatology and float-based flux during prolonged positive SAM conditions in 2015–2016 suggests an influence of measurement bias during those years or the possibility that the ship-based climatology does not constrain increased upwelling of CO_2-rich water in higher latitudes. Sustained observations are needed to better constrain interannual variability like the anomalous strong winter outgassing observed by floats in 2015–2016 relative to 2017–2019. Better coverage of ships, USVs, and floats are needed to resolve these uncertainties in measurements and variability in the Southern Ocean.

4. Conclusions

Climate change is predicted to reduce ocean CO_2 uptake under climate model scenarios that show intensification of winds and acceleration of the overturning circulation in the Southern Ocean (Le Quéré et al., 2007). Over the next century models also predict reductions in sea-ice cover and surface ocean warming, freshening, and stratification, which are all expected to impact the carbon sink. How these processes impact the overall balance of CO_2 outgassing and uptake in the Southern Ocean is uncertain. Better representation of these processes in models is necessary to predict the Southern Ocean's role in a future climate.

Our results indicate that the strong wintertime outgassing observed by floats in 2015 and 2016 was not prevalent in 2019. The change may be linked to a decline in the SAM index in the later years leading to a reduction in upwelling of CO_2 rich waters to the surface. More sustained observations are needed to constrain interannual variability and the impact on both Southern Ocean and global ocean CO_2 uptake estimates. The first circumnavigation of the Southern Ocean by a USV described here has shown the capability to collect high quality data that can be used to constrain multiplatform measurement uncertainties and interrogate how variability from the scale of hours to years may impact CO_2 flux estimates.

A multiplatform observing network consisting of USVs directly surveying air-sea interactions, floats measuring full water column biogeochemistry even under ice, and the ship-based measurements for ground-truthing autonomous sensors would, in combination, best track changes in ocean carbon uptake and better constrain variability. USVs fill a unique niche with the ability to survey regions for extended periods where ships do not routinely operate, opening up new opportunities for filling persistent gaps in the ocean observing system with high-quality pCO$_2$ and meteorological observations.

Data Availability Statement

The USV data used here are available at https://doi.org/10.25921/6zja-cg56 (Sutton et al., 2020). Data are available through Sutton et al., 2020.

References

Bushinsky, S. M., Landschützer, P., Rödenbeck, C., Gray, A. R., Baker, D., Mazloff, M. R., et al. (2019). Reassessing Southern Ocean air-sea CO_2 flux estimates with the addition of biogeochemical float observations. *Global Biogeochemical Cycles*, *33*(11), 1370–1388. https://doi.org/10.1029/2019GB006176

Chiodi, A. M., Dunne, J. P., & Harrison, D. E. (2019). Estimating air-sea carbon flux uncertainty over the tropical Pacific: Importance of winds and wind analysis uncertainty. *Global Biogeochemical Cycles*, *33*(3), 370–390. https://doi.org/10.1029/2018GB006047

Cronin, M. F., Gentemann, C. L., Edson, J., Ueki, I., Bourassa, M., Brown, S., et al. (2019). Air-sea fluxes with a focus on heat and momentum. *Frontiers in Marine Science*, *6*, 430. https://doi.org/10.3389/fmars.2019.00430

Cronin, M. F., Meinig, C., Sabine, C. L., Ichikawa, H., & Tomita, H. (2008). Surface mooring network in the Kuroshio Extension. *IEEE Systems Journal*, *2*(3), 424–430.

Dee, D. P., Uppala, S. M., Simmons, A. J., Berrisford, P., Poli, P., Kobayashi, S., et al. (2011). The ERA-Interim reanalysis: Configuration and performance of the data assimilation system. *Quarterly Journal of the Royal Meteorological Society*, *137*(656), 553–597. https://doi.org/10.1002/qj.828

Dickson, A. G., Sabine, C. L., & Christian, J. R. (Eds.), (2007). *Guide to best Practices for ocean CO_2 measurements* (pp. 191). PICES Special Publication 3.

Dlugokencky, E. G., Thoning, K. W., Lang, P. M., & Tans, P. P. (2019). *NOAA greenhouse gas reference from atmospheric carbon dioxide dry air mole fractions from the NOAA ESRL carbon cycle cooperative global air sampling network*. Retrieved from ftp://aftp.cmdl.noaa.gov/data/trace_gases/co2/flask/surface/

Fay, A. R., McKinley, G. A., & Lovenduski, N. S. (2014). Southern Ocean carbon trends: Sensitivity to methods. *Geophysical Research Letters*, *41*(19), 6833–6840. https://doi.org/10.1002/2014GL061324

Frölicher, T. L., Sarmiento, J. L., Paynter, D. J., Dunne, J. P., Krasting, J. P., & Winton, M. (2014). Dominance of the Southern Ocean in anthropogenic carbon and heat uptake in CMIP5 models. *Journal of Climate*, *28*(2), 862–886. https://doi.org/10.1175/JCLI-D-14-00117.1

Gray, A. R., Johnson, K. S., Bushinsky, S. M., Riser, S. C., Russell, J. L., Talley, L. D., et al. (2018). Autonomous biogeochemical floats detect significant carbon dioxide outgassing in the high-latitude Southern Ocean. *Geophysical Research Letters*, *45*(17), 9049–9057. https://doi.org/10.1029/2018GL078013

Hersbach, H., Bell, B., Berrisford, P., Hirahara, S., Horányi, A., Muñoz-Sabater, J., et al. (2020). The ERA5 global reanalysis. *Quarterly Journal of the Royal Meteorological Society Skip*, *146*(730), 1999–2049.

Hihara, T., Kubota, M., & Okuro, A. (2015). Evaluation of sea surface temperature and wind speed observed by GCOM-W1/AMSR2 using in situ data and global products. *Remote Sensing of Environment*, *164*, 170–178. https://doi.org/10.1016/j.rse.2015.04.005

Iudicone, D., Rodgers, K. B., Stendardo, I., Aumont, O., Madec, G., Bopp, L., et al. (2011). Water masses as a unifying framework for understanding the Southern Ocean carbon cycle. *Biogeosciences*, *8*(5), 1031–1052. https://doi.org/10.5194/bg-8-1031-2011

Johnson, K. S., Riser, S. C., Boss, E. S., Talley, L. D., Sarmiento, J. L., Swift, D. D., et al. (2020). SOCCOM float data—Snapshot 2020-08-30 In *Southern Ocean carbon and climate observations and modeling (SOCCOM) float data archive* UC San Diego Library Digital Collections. https://doi.org/10.6075/J0BK19W5

Kanamitsu, M., Ebisuzaki, W., Woollen, J., Yang, S.-K., Hnilo, J. J., Fiorino, M., & Potter, G. L. (2002). NCEP–DOE AMIP-II Reanalysis (R-2). *Bulletin of the American Meteorological Society*, *83*(11), 1631–1644. https://doi.org/10.1175/BAMS-83-11-1631

Kent, E. C., Fangohr, S., & Berry, D. I. (2013). A comparative assessment of monthly mean wind speed products over the global ocean. *International Journal of Climatology*, *33*(11), 2520–2541. https://doi.org/10.1002/joc.3606

Keppler, L., & Landschützer, P. (2019). Regional wind variability modulates the Southern Ocean carbon sink. *Scientific Reports*, *9*(1), 7384. https://doi.org/10.1038/s41598-019-43826-y

Khatiwala, S., Primeau, F., & Hall, T. (2009). Reconstruction of the history of anthropogenic CO_2 concentrations in the ocean. *Nature*, *462*(7271), 346–349. https://doi.org/10.1038/nature08526

Kubota, M., Iwabe, N., Cronin, M. F., & Tomita, H. (2008). Surface heat fluxes from the NCEP/NCAR and NCEP/DOE reanalyzes at the KEO buoy site. *Journal of Geophysical Research*, *113*, C02009. https://doi.org/10.1029/2007JC004338 Retrieved from https://agupubs.onlinelibrary.wiley.com/doi/full/10.1029/2007JC004338

Landschützer, P., Gruber, N., & Bakker, D. C. E. (2016). Decadal variations and trends of the global ocean carbon sink. *Global Biogeochemical Cycles*, *30*(10), 1396–1417. https://doi.org/10.1002/2015GB005359

Landschützer, P., Gruber, N., Bakker, D. C. E., & Schuster, U. (2014). Recent variability of the global ocean carbon sink. *Global Biogeochemical Cycles*, *28*(9), 927–949. https://doi.org/10.1002/2014GB004853

Landschützer, P., Gruber, N., Haumann, F. A., Rödenbeck, C., Bakker, D. C. E., van Heuven, S., et al. (2015). The reinvigoration of the Southern Ocean carbon sink. *Science*, *349*(6253), 1221–1224. https://doi.org/10.1126/science.aab2620

Landschützer, P., Gruber, N., & Bakker, D. C. E. (2020). *An observation-based global monthly gridded sea surface pCO_2 product from 1982 onward and its monthly climatology (NCEI Accession 0160558)*. Dataset. NOAA National Centers for Environmental Information. https://doi.org/10.7289/V5Z899N6

Le Quéré, C., Rödenbeck, C., Buitenhuis, E. T., Conway, T. J., Langenfelds, R., Gomez, A., et al. (2007). Saturation of the Southern Ocean CO_2 sink due to recent climate change. *Science*, *316*(5832), 1735–1738. https://doi.org/10.1126/science.1136188

Lovenduski, N. S., Fay, A. R., & McKinley, G. A. (2015). Observing multidecadal trends in Southern Ocean CO_2 uptake: What can we learn from an ocean model? *Global Biogeochemical Cycles*, *29*(4), 416–426. https://doi.org/10.1002/2014GB004933

Lovenduski, N. S., Gruber, N., & Doney, S. C. (2008). Toward a mechanistic understanding of the decadal trends in the Southern Ocean carbon sink. *Global Biogeochemical Cycles*, *22*(3), GB3016. https://doi.org/10.1029/2007GB003139

Lovenduski, N. S., Gruber, N., Doney, S. C., & Lima, I. D. (2007). Enhanced CO_2 outgassing in the Southern Ocean from a positive phase of the Southern Annular Mode. *Global Biogeochemical Cycles*, *21*(2), GB2026. https://doi.org/10.1029/2006GB002900

Marshall, G. J. (2003). Trends in the Southern Annular Mode from observations and reanalyzes. *Journal of Climate*, *16*(24), 4134–4143. https://doi.org/10.1175/1520-0442%282003%29016%3C4134%3ATITSAM%3E2.0.CO%3B2

Mears, C. A., Scott, J., Wentz, F. J., Ricciardulli, L., Leidner, S. M., Hoffman, R., & Atlas, R. (2019). A near-real-time version of the Cross-Calibrated Multiplatform (CCMP) ocean surface wind velocity data set. *Journal of Geophysical Research: Oceans*, *124*(10), 6997–7010. https://doi.org/10.1029/2019JC015367

Meinig, C., Burger, E. F., Cohen, N., Cokelet, E. D., Cronin, M. F., Cross, J. N., et al. (2019). Public–private partnerships to advance regional ocean-observing capabilities: A Saildrone and NOAA-PMEL case study and future considerations to expand to global scale observing. *Frontiers in Marine Science*, *6*, 448. https://doi.org/10.3389/fmars.2019.00448

Monteiro, P. M. S., Gregor, L., Lévy, M., Maenner, S., Sabine, C. L., & Swart, S. (2015). Intraseasonal variability linked to sampling alias in air-sea CO_2 fluxes in the Southern Ocean. *Geophysical Research Letters*, *42*(20), 8507–8514. https://doi.org/10.1002/2015GL066009

Nevison, C. D., Munro, D. R., Lovenduski, N. S., Keeling, R. F., Manizza, M., Morgan, E. J., & Rödenbeck, C. (2020). Southern Annular Mode influence on wintertime ventilation of the Southern Ocean detected in atmospheric O_2 and CO_2 measurements. *Geophysical Research Letters*, *47*(20), e2019GL085667. https://doi.org/10.1029/2019GL085667

Orsi, A. H., Whitworth, T., & Nowlin, W. D. (1995). On the meridional extent and fronts of the Antarctic Circumpolar Current. *Deep Sea Research Part I: Oceanographic Research Papers*, *42*(5), 641–673. https://doi.org/10.1016/0967-0637(95)00021-W

Pierrot, D., Neill, C., Sullivan, K., Castle, R., Wanninkhof, R., Lüger, H., et al. (2009). Recommendations for autonomous underway pCO_2 measuring systems and data-reduction routines. *Deep Sea Research Part II: Topical Studies in Oceanography*, *56*(8–10), 512–522. https://doi.org/10.1016/j.dsr2.2008.12.005

Rödenbeck, C., Bakker, D. C. E., Gruber, N., Iida, Y., Jacobson, A. R., Jones, S., et al. (2015). Data-based estimates of the ocean carbon sink variability—First results of the Surface Ocean pCO2 Mapping intercomparison (SOCOM). *Biogeosciences*, *12*(23), 7251–7278.

Roobaert, A., Laruelle, G. G., Landschützer, P., & Regnier, P. (2018). Uncertainty in the global oceanic CO_2 uptake induced by wind forcing: quantification and spatial analysis. *Biogeosciences*, *15*(6), 1701–1720. https://doi.org/10.5194/bg-15-1701-2018

Sabine, C., Sutton, A., McCabe, K., Lawrence-Slavas, N., Alin, S., Feely, R., et al. (2020). Evaluation of a new carbon dioxide system for autonomous surface vehicles. *Journal of Atmospheric and Oceanic Technology*, *37*(8), 1305–1317. https://doi.org/10.1175/JTECH-D-20-0010.1

Sutton, A. J., Battisti, R., Maenner Jones, S., Musielewicz, S., Bott, R., & Osborne, J. (2020). *Surface underway measurements of partial pressure of carbon dioxide (pCO_2), sea surface temperature, sea surface salinity and other parameters from Autonomous Surface Vehicle ASV_Saildrone1020 (EXPOCODE 32DB20190119) in the South Atlantic Ocean, South Pacific Ocean, Indian Ocean and Southern Ocean from 2019-01-19 to 2019-08-03 (NCEI Accession 0221912)*: NOAA National Centers for Environmental Information. https://doi.org/10.25921/6zja-cg56

Sutton, A. J., Sabine, C. L., Maenner-Jones, S., Lawrence-Slavas, N., Meinig, C., Feely, R. A., et al. (2014). A high-frequency atmospheric and seawater pCO_2 data set from 14 open-ocean sites using a moored autonomous system. *Earth System Science Data*, *6*(2), 353–366. https://doi.org/10.5194/essd-6-353-2014

Sutton, A. J., Wanninkhof, R., Sabine, C. L., Feely, R. A., Cronin, M. F., & Weller, R. A. (2017). Variability and trends in surface seawater pCO$_2$ and CO$_2$ flux in the Pacific Ocean. *Geophysical Research Letters*, *44*(11), 5627–5636. https://doi.org/10.1002/2017GL073814

Takahashi, T., Sutherland, S. C., Wanninkhof, R., Sweeney, C., Feely, R. A., Chipman, D. W., et al. (2009). Climatological mean and decadal change in surface ocean pCO$_2$, and net sea-air CO$_2$ flux over the global oceans. *Deep Sea Research Part II: Topical Studies in Oceanography*, *56*(8–10), 554–577. https://doi.org/10.1016/j.dsr2.2008.12.009

Takahashi, T., Sweeney, C., Hales, B., Chipman, D. W., Newberger, T., Goddard, J. G., et al. (2012). The changing carbon cycle in the Southern Ocean. *Oceanography*, *25*(3), 26–37.

Tomita, H., Kawai, Y., Cronin, M. F., Hihara, T., & Kubota, M. (2015). Validation of AMSR2 sea surface wind and temperature over the Kuroshio Extension region. *Scientific Online Letters on the Atmosphere*, *11*, 43–47.

Wallcraft, A. J., Kara, A. B., Barron, C. N., Metzger, E. J., Pauley, R. L., & Bourassa, M. A. (2009). Comparisons of monthly mean 10 m wind speeds from satellites and NWP products over the global ocean. *Journal of Geophysical Research*, *114*(D16). D16109. https://doi.org/10.1029/2008JD011696

Wanninkhof, R. (2014). Relationship between wind speed and gas exchange over the ocean revisited. *Limnology and Oceanography: Methods*, *12*(6), 351–362. https://doi.org/10.4319/lom.2014.12.351

Weiss, R. F. (1974). Carbon dioxide in water and seawater: the solubility of a non-ideal gas. *Marine Chemistry*, *2*(3), 203–215. https://doi.org/10.1016/0304-4203(74)90015-2

Weissman, D. E., Stiles, B. W., Hristova-Veleva, S. M., Long, D. G., Smith, D. K., Hilburn, K. A., & Jones, W. L. (2012). Challenges to satellite sensors of ocean winds: Addressing precipitation effects. *Journal of Atmospheric and Oceanic Technology*, *29*(3), 356–374. http://doi.org/10.1175/JTECH-D-11-00054.1

Weller, R. A. (2015). Variability and trends in surface meteorology and air–sea fluxes at a site off northern Chile. *Journal of Climate*, *28*(8), 3004–3023. https://doi.org/10.1175/JCLI-D-14-00591.1

Williams, N. L., Juranek, L. W., Feely, R. A., Johnson, K. S., Sarmiento, J. L., Talley, L. D., et al. (2017). Calculating surface ocean pCO$_2$ from biogeochemical Argo floats equipped with pH: An uncertainty analysis. *Global Biogeochemical Cycles*, *31*(3), 591–604. https://doi.org/10.1002/2016GB005541

Zhang, D., Cronin, M. F., Meinig, C., Farrar, J. T., Jenkins, R., Peacock, D., et al. (2019). Comparing air-sea flux measurements from a new unmanned surface vehicle and proven platforms during the SPURS-2 field campaign. *Oceanography*, *32*(2), 122–133. https://doi.org/10.5670/oceanog.2019.220

References From the Supporting Information

Large, W. G., & Pond, S. (1981). Open ocean momentum flux measurements in moderate to strong winds. *Journal of Physical Oceanography*, *11*(3), 324–336. https://doi.org/10.1175/1520-0485(1981)011<0324:OOMFMI>2.0.CO;2

Watson, A. J., Schuster, U., Shutler, J. D., Holding, T., Ashton, I. G. C., Landschützer, P., et al. (2020). Revised estimates of ocean-atmosphere CO2 flux are consistent with ocean carbon inventory. *Nature Communications*, *11*(1), 4422. https://doi.org/10.1038/s41467-020-18203-3

Weiss, R. F., Jahnke, R. A., & Keeling, C. D. (1982). Seasonal effects of temperature and salinity on the partial pressure of CO$_2$ in seawater. *Nature*, *300*(5892), 511–513. https://doi.org/10.1038/300511a0